Integrated wavelength-selective optical waveguides for microfluidic-based laser-induced fluorescence detection

Christopher L. Bliss, James N. McMullin† and Christopher J. Backhouse†*

Received 31st July 2007, Accepted 16th October 2007
First published as an Advance Article on the web 31st October 2007
DOI: 10.1039/b711601b

We demonstrate the fabrication and characterization of a novel, inexpensive microchip capable of laser induced fluorescence (LIF) detection using integrated waveguides with built-in optical filters. Integrated wavelength-selective optical waveguides are fabricated by doping poly(dimethysiloxane) (PDMS) with dye molecules. Liquid-core waveguides are created within dye-doped PDMS microfluidic chips by filling channels with high refractive index liquids. Dye molecules are allowed to diffuse into the liquid core from the surrounding dye-doped PDMS. The amount of diffusion is controlled by choosing either polar (low diffusion) or apolar (high diffusion) liquid waveguide cores. The doping dye is chosen to absorb excitation light and to transmit fluorescence emitted by the sample under test. After 24 h, apolar waveguides demonstrate propagation losses of 120 dB cm^{-1} (532 nm) and 4.4 dB cm^{-1} (633 nm) while polar waveguides experience losses of 8.2 dB cm^{-1} (532 nm) and 1.1 dB cm^{-1} (633 nm) where 532 and 633 nm light represent the excitation and fluorescence wavelengths, respectively. We demonstrate the separation and detection of end-labelled DNA fragments using polar waveguides for excitation light delivery and apolar waveguides for fluorescence collection. We demonstrate that the dye-doped waveguides can provide performance comparable to a commercial dielectric filter; however, for the present choice of dye, their ultimate performance is limited by autofluorescence from the dye. Through the detection of a BK virus polymerase chain reaction (PCR) product, we demonstrate that the dye-doped PDMS system is an order of magnitude more sensitive than a similar undoped system (SNR: 138 *vs.* 9) without the use of any external optical filters at the detector.

1 Introduction

The integration of optical filters into fluorescence-based lab-on-a-chip (LOC) systems is key in reducing the size and cost of the detection optics. This enables the development of point-of-care diagnostic systems while retaining adequate sensitivity for a clear diagnosis. Dandin *et al.* recently provided a comprehensive review on optical filtering technologies for integrated fluorescence sensors.[1] Reflective interference filters are common in applications involving photodetector integration.[2–8] However, the fabrication of such multilayer optical filters requires large numbers of alternating layers to achieve adequate attenuation.[6] Additionally, these filters are incident angle-dependent and require collimation optics for efficient light filtering.

Alternatively, absorptive (or colour) filters have been used by several groups.[9–11] Absorbance-based filters are inexpensive to fabricate and the strength of the filter is not sensitive to the incident angle. Hofmann *et al.* have recently demonstrated an interesting and cost-effective approach to integrate a long-pass absorptive filter on-chip by doping bulk PDMS with lysochrome dyes.[9] In that work, Hofmann *et al.* produce and characterize featureless sheets of dye-doped PDMS. While the demonstrated dye-doped slab filters displayed good performance, the monolithic detection scheme proposed by Hofmann presents a significant practical challenge. This monolithic fluorescence detection scheme consists of a microfluidic chip sandwiched between an LED and a photodetector. However, unless the optical attenuation provided by the dye-doped PDMS is very strong, this configuration will saturate the photodetector with excitation light. Unfortunately, the maximum optical density of the integrated filter is restricted since the quantity of dye that can be incorporated into the PDMS matrix is limited by both the solubility of the dye in toluene and the volume of toluene that can be added to the PDMS without inhibiting curing. This means that an increase in optical density requires an increase in filter thickness.

With this in mind, the monolithic detection scheme requires a compromise between excitation light suppression and fluorescence collection. An increase in optical density will require an increase in filter thickness, but an increased filter thickness implies a greater distance between the sample and photodetector resulting in a reduction in the light collection efficiency (LCE) of the detector (the fraction of sample fluorescence that reaches the detector). For example, Chabinyc *et al.* reported a LCE of only 0.2% by a 30 μm diameter avalanche photodiode at a distance of only 200 μm from the channel system.[10] The LCE would be further reduced to ~0.005% at 1 mm.

We have recently demonstrated a liquid-core waveguide-based excitation and detection scheme for laser-induced

Department of Electrical and Computer Engineering, University of Alberta, Edmonton, Alberta, Canada. E-mail: chrisb@ualberta.ca; Fax: +1 (780) 492-1811; Tel: +1 (780) 492-2920
† These authors contributed equally to this work.

fluorescence (LIF) with performance comparable to a commercial confocal system.[12] Our goal is to integrate the entire diagnostic system while minimizing the device cost and a significant challenge is to integrate the optical filter, a critical component in LIF systems. An effective solution would be to integrate the optical filter directly into the fluorescence collection waveguide. Unlike the system developed by Hofmann *et al.*, the optical density of the filter could be increased without reducing the LCE of the detection optics by increasing the length of the waveguide since the waveguide numerical aperture remains constant.

The Whitesides group has demonstrated the use of liquid-core waveguides containing dissolved dyes to isolate particular wavelength ranges from a single white light source using a diffusion-controlled waveguide splitter.[13] However, this integrated filter technology has not yet been applied to fluorescence detection.

Yin *et al.* demonstrate integrated filter functionality using liquid-core ARROW waveguides, which selectively confine particular wavelengths within a low index core by tailoring the design of the Fabry–Perot cladding.[14] However, ARROW waveguides are inherently ''leaky'' and require additional reflecting layers to decrease the propagation loss. While this technique provides a high degree of flexibility in terms of tuning the optical passband and stopband, deposition of the alternating dielectric layers that form the cladding is time consuming and expensive and therefore the ARROW waveguide is not a likely candidate for integration onto a disposable lab-on-a-chip (LOC) device.

In an extension to our previous work and the work of Hofmann *et al.*, we report the integration of dye-doped PDMS into our waveguide-based microfluidic DNA analysis device to create novel wavelength-selective waveguides which rely on diffusion to ''pull'' dye out of the bulk material into the waveguide core. The dye is chosen such that the detection waveguide selectively attenuates stray excitation light, while efficiently transmitting the fluorescence signal. Since the bulk chip material consists of dye-doped PDMS, it rapidly absorbs any reflected or scattered excitation light preventing this light from reaching the detector. This provides an advantage over simply creating a waveguide core containing a dissolved dye within an undoped PDMS chip. The use of dye-doped PDMS as an absorbing waveguide effectively eliminates the requirement for an interference filter at the detector since signal collection and noise suppression are both performed using the same element. At the time of writing, the present work was the first demonstration of the use of waveguides containing dissolved dyes as a detection filter for fluorescence sensing applications. (We note the very recent publication of related work by Lee *et al.*)[15]

Scattered excitation light is present in all LIF systems resulting in an increased signal baseline and shot noise at the detector. The system reported in this work dramatically reduces the effects of stray excitation light through three effects: (i) the dye-doped bulk material in the chip is strongly absorbing at the excitation wavelength and scattered excitation light is quickly absorbed before it can be collected by the detection waveguide; (ii) the detection waveguide is placed at an angle of 45° to the excitation waveguide acting as a spatial filter to prevent direct coupling of excitation light into the detection waveguide; (iii) excitation light collected by the detection waveguide is absorbed by dye molecules which have diffused from the bulk PDMS into the liquid core of the waveguide, while the fluorescence from the sample is delivered to the detector with much less attenuation.

The microfluidic devices are fabricated though PDMS soft lithography. However, a toluene-dye solution is mixed with the uncured PDMS prior to casting to create dye-doped PDMS. Following chip fabrication (after curing and bonding), two types of waveguides are formed by adding high refractive index liquids into dedicated channels within the chip. High performance, wavelength-selective, attenuating waveguides are formed by using a liquid PDMS pre-polymer as the core material. In this case, the liquid core is miscible with other apolar liquids so residual toluene from the bulk chip, including the dissolved dye, is free to diffuse from the bulk PDMS into the core. The high performance attenuating waveguides are used for detection since a high dye concentration in the waveguide core will result in high attenuation of the unwanted excitation light. The use of a more polar liquid will limit the diffusion of dye into the core and will thus reduce the waveguide attenuation strength. Excitation waveguides are filled with a polar liquid (glycerol) to reduce dye diffusion into the core, allowing excitation light to reach the sample with minimal attenuation. The proposed system eliminates the requirement for nearly all external passive optics, while maintaining an excellent SNR.

In the next section, we describe the microfluidic chip design, fabrication procedure and waveguide propagation properties. In Section 3, we demonstrate the effectiveness of the wavelength-selective waveguide as an integrated optical filter. We achieve this through the analysis of BK virus (BKV) DNA fragments, obtained through polymerase chain reaction (PCR) with end-labelled primers, using our custom microchip electrophoresis system. We compare the sensitivity, in terms of SNR, to similar experiments performed using an undoped PDMS microchip with traditional, non-attenuating waveguides and a commercial external interference filter placed in-line with the photodetector. We show that an external interference filter is required to allow reliable detection of BKV when using an undoped, colourless PDMS microchip. However, when the external interference filter is removed, we show that dye-doped microchips containing attenuating waveguides can provide clear detection of the PCR product and compare well in terms of sensitivity to results obtained using an undoped chip with the external filter. Thus, the wavelength-selective waveguides are an effective replacement of the external optical filter and represent a significant step toward miniaturizing the entire optical system.

2 Results and discussion

2.1 Device fabrication

The microfluidic devices (Fig 1A) were fabricated through PDMS soft lithography, as described elsewhere,[12] modified to allow the incorporation of lysochrome dye into the bulk material. The uniform dispersal of lysochrome dye molecules into PDMS and subsequent optical transmission properties

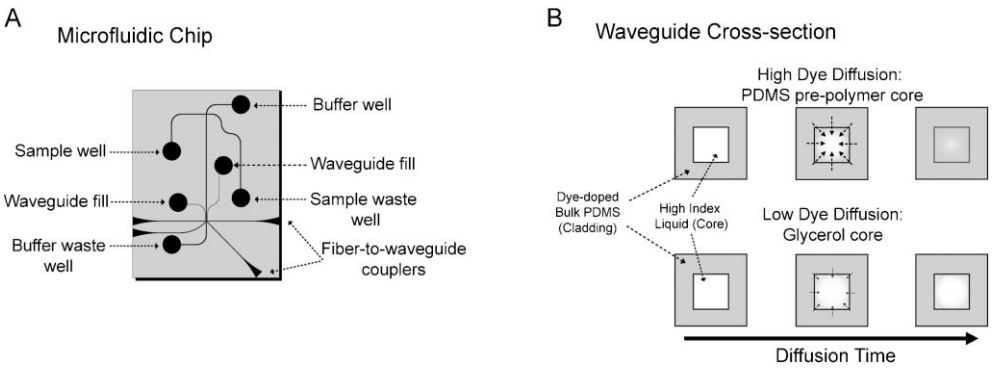

Fig. 1 (A) A schematic of the dye-doped PDMS microfluidic device. (B) A cross-sectional view of the two types of dye-doped waveguides. Waveguides filled with PDMS pre-polymer experience higher dye diffusion into the core since toluene and the dye are soluble in the pre-polymer, resulting in a stronger optical filter effect. Since toluene and the dye are relatively insoluble in glycerol, glycerol filled waveguides experience less dye diffusion and weaker optical filter effects.

has been reported previously by Hofmann *et al.*[9] Briefly, the PDMS pre-polymer and curing agent (Sylgard 184, Dow Corning, NC, USA) were mixed at a 10 : 1 (w/w) ratio. Sudan II dye (Sigma-Aldrich, MO, USA) was then dissolved in toluene and the solution was added to the PDMS mixture followed by thorough mixing. In order to ensure complete curing of the PDMS, the toluene content was restricted to below 10% (v/v).[9] Concentrations of 1200 μg mL^{-1}, the optimum dye loading as determined by Hofmann *et al.*, were formed by adding 19.8 mg of Sudan II dye to 1 mL of toluene and 16.5 g of the PDMS. The PDMS mixture was degassed for 30 min under vacuum prior to pouring onto the master and curing at 80 °C for 4 h. To form microfluidic devices, featureless PDMS slabs fabricated in a similar fashion were bonded to the PDMS replica mould after treatment with an oxygen plasma. Colourless PDMS microchips, containing no toluene or Sudan II dye, were fabricated as well for comparison purposes.

Refractive index measurements were performed to ensure that the addition of toluene (n = 1.50) or Sudan II dye did not modify the refractive index of the bulk PDMS. This could possibly prohibit light confinement in the waveguides if the refractive index was increased beyond that of the core material. Samples of unmodified PDMS, PDMS containing toluene and PDMS containing both toluene and Sudan II were spun onto a silicon substrate at 6100 rpm for 30 s. The PDMS films were approximately 6 μm thick. The PDMS was prepared and cured as previously described. The refractive index of each sample was measured to be 1.410 $\pm$ 0.005 at 633 nm using the prism coupling method (Model 2010 Prism Coupler, Metricon Corp., NJ, USA), thus the PDMS dye-doping protocol has a negligible impact on the refractive index. The waveguide cores were formed by adding either PDMS pre-polymer (OE-43-Part B, Gelest, PA, USA) or glycerol to microfluidic channels fabricated within the bulk PDMS. The refractive index of glycerol is 1.47 and the refractive index of uncured pre-polymer was measured to be 1.429 $\pm$ 0.002 at 589 nm using a Bausch and Lomb 33-45-58 Abbe-type refractometer.

We predicted that we would observe light attenuation through one of three mechanisms: (i) dye would diffuse from the bulk PDMS into the core material resulting in increased attenuation as a function of increased concentration or diffusion time; (ii) the high refractive index liquid core material would diffuse into the bulk PDMS creating a graded-index effect. Light would begin to travel in regions of the bulk material that had absorbed the high index liquid and the dye in the bulk material would absorb light, increasing the waveguide attenuation; (iii) evanescent interaction between the guided light and the dye-doped cladding would result in light attenuation. While we expected (iii) to dominate, we noticed an increase in attenuation with time suggesting that diffusion effects were dominating. This time dependence is described in detail in the next section. We discounted (ii) since an image of the waveguide cross section (not shown) indicated very little light propagation in regions beyond the fabricated waveguide boundaries. We concluded that a significant portion of the waveguide attenuation is a result of light absorption by dye which has diffused from the bulk dye-doped PDMS into the liquid waveguide core. This conclusion was supported by the observation of an orange hue in the pre-polymer core material upon removal from the waveguide. As shown in Fig 1B, the strength of the filter can be adjusted by controlling the rate of dye diffusion into the core. Since the Sudan II dye is more soluble in non-polar liquids, the strength of the filter is enhanced by using a non-polar liquid (PDMS pre-polymer) or minimized by using a polar liquid (glycerol) as a core material. It is also possible that the dye-doping of the core is dominated by the diffusion of residual toluene (and dissolved dyes) from the bulk PDMS into the liquid core rather than by the diffusion of the dye itself.

2.2 Wavelength-selective waveguide characterization

The transmission spectrum of the dye-doped PDMS was determined using a PerkinElmer Lambda 900 UV/VIS/NIR spectrophotometer (PerkinElmer, MA, USA). Data was collected at 1 nm resolution over a range of 350–850 nm with a slit width of 1 nm. The PMT integration time was set to 2 s to obtain a large enough SNR such that the minimum measurable transmittance was 0.001%. Transmission measurements were performed on featureless dye-doped PDMS samples with thicknesses of approximately 1 mm at dye loadings of 720 μg mL^{-1} and 1200 μg mL^{-1} in reference to air

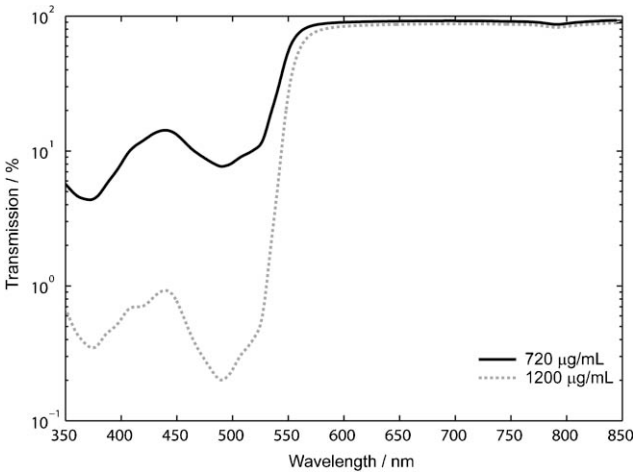

Fig. 2 The transmission spectrum of 1 mm dye-doped PDMS. The quality factor of the optical filter increases by an order of magnitude (Q = 6 to 66) when the dye concentration in the PDMS is increased from 720 μg mL^{-1} to 1200 μg mL^{-1}.

(Fig. 2). The filter quality is assessed using the figure of merit $Q = T(\lambda_{transmit})/T(\lambda_{block})$, as defined by Hofmann *et al.*,[9] where $T(\lambda_{transmit})$ and $T(\lambda_{block})$ represent the % transmission through the filter at a wavelength above and below the filter cut-off, respectively. In this work, the figure of merit Q is determined at $\lambda_{transmit}$ = 633 nm and λ_{block} = 532 nm. We achieve a Q of 6 and 66 for samples with dye loadings of 720 μg mL^{-1} and 1200 μg mL^{-1}, respectively. A more thorough approximation to the filter quality would consider the wavelength dependence of the filter spectrum along with the excitation and fluorescence spectra as described in ref. 9, but the simplified model provides a reasonable estimate of the filter quality.

As previously mentioned, guided-mode waveguides are formed through the addition of high index liquids into microfluidic channels. In the case of the high performance attenuating waveguides, the PDMS pre-polymer core is initially colourless with low absorption at visible wavelengths. However, dye molecules quickly diffuse into the pre-polymer core from the dye-doped bulk PDMS creating an attenuating waveguide with transmission properties similar to those described above. Dye diffusion cannot be completely avoided by using glycerol and thus the low-loss waveguides still absorb light according to the above spectral curve, but to a lesser extent due to the lower uptake by the polar glycerol.

The optical filter strength is determined by measuring the waveguide propagation loss at 532 nm and 633 nm to represent wavelengths in the stopband and the passband of the optical filter, respectively. Approximately 2 mW of light from either a red or green laser diode is coupled into the waveguide and scattered light is collected at 90° using a 1 mm plastic optical fiber at several positions along the waveguide.[12] If we assume that the density of light scattering centers, due to fabrication defects or waveguide core impurities, is roughly constant throughout the length of the waveguide, light scattered from the waveguide is proportional to the power of the confined light. In order to monitor the effects of diffusion on the waveguide attenuation, we also studied the waveguide loss as a function of time. A summary of the per unit length waveguide attenuation results are tabulated in Table 1.

As expected, we observe similar waveguide propagation losses at both 532 nm and 633 nm when using the colourless, undoped PDMS waveguides with OE-43-B PDMS pre-polymer cores. This was consistent with the idea that losses were primarily a result of scattering by surface roughness on the waveguide walls. However, very little scattered light was observed when using glycerol and we could not observe any measurable loss using our current measurement technique. The decreased performance of the PDMS pre-polymer in comparison to glycerol is thought to be due to additional light scattering from the PDMS pre-polymer, possibly due to scattering from the PDMS monomers. This may also explain why, when using the PDMS pre-polymer core, we typically observe a slightly higher propagation loss ($\sim$1 dB cm^{-1}) at 532 nm since the degree of scattering for a particular wavelength is known to be dependent on the physical size of the scatterer.[16]

The waveguides formed in microfluidic chips fabricated using dye-doped PDMS exhibit significant attenuation due to Sudan II dye diffusion into the waveguide core. The measured time-dependant waveguide attenuation, $\alpha(t)$, fits a model of the form $\alpha(t) = \alpha_0 + \alpha_1(1 - e^{-t/\tau})$, where the time constant, τ, was determined to be 33 h for waveguides containing PDMS pre-polymer and 6700 h for waveguides containing glycerol. However, this model does not accurately explain the rapid increase in attenuation from the expected initial value (similar to waveguide attenuation measured in un-doped PDMS) to the

Table 1 Measured waveguide attenuation

Bulk material (cladding)	Core material	Diffusion time/h	Waveguide attenuation/dB cm^{-1}	
			532 nm	633 nm
Undoped PDMS	OE-43-B	—	2.9	2.2
	Glycerol	—	[a]	[a]
Sudan-doped PDMS (1200 μg mL^{-1})	OE-43-B	1	118	3.3
		3	120	3.5
		24	120	4.4
		48	120	4.9
	Glycerol	1	7.6	[a]
		3	6.5	0.2
		24	8.2	1.1
		48	9.8	1.0

[a] Loss too small to measure using our current setup.

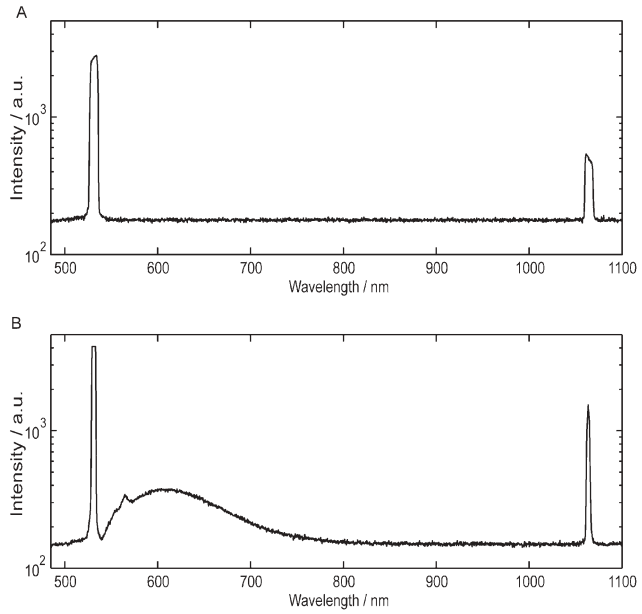

Fig. 3 A comparison between the spectrum of (A) a green diode laser and (B) the output of a 3 mm dye-doped waveguide excited using the same laser on a logarithmic scale as measured by a fiber-coupled spectrometer (USB2000, Ocean Optics, FL, USA). The absolute intensity of the light collected by the spectrometer is different for (A) and (B). However, information on the spectral content can be obtained by comparing the relative intensity of the light at each wavelength. The primary laser diode emission at 532 nm is frequency doubled from a 1064 nm Nd:YAG laser and a significant component at 1064 nm is still present after passing through an IR filter. Significant autofluorescence generated from the Sudan II dye is observed between 550–750 nm.

waveguide attenuation measured after 1 h. This suggests that the waveguide initially experiences rapid diffusion followed by a period of slower diffusion. We believe that once the dye embedded near the surface of the waveguide channel is depleted, the diffusion becomes rate-limited by dye diffusion from the bulk PDMS to the surface of the waveguide channel.

In contrast to the observations of Hofmann *et al.*, we noticed considerable autofluorescence from the Sudan-doped PDMS. This is particularly apparent when we compare the spectrum of the emission from a green laser diode (Fig. 3A) to the output of a 3 mm long dye-doped waveguide (Fig. 3B) excited using the same laser. After passing the excitation light through the short waveguide, we see spectral content in the region between 550–750 nm due to autofluorescence of the Sudan II dye. Since the device has been designed to absorb both excitation light that is confined to the detection waveguide and scattered excitation light which has entered the bulk PDMS substrate, both the dye-doped PDMS substrate and the dye molecules in the liquid core contribute to the autofluorescence.

The waveguide propagation loss is determined from the slope of the decay in intensity along the dye-doped waveguides, as shown in Fig. 4. When 532 nm light is coupled into a dye-doped waveguide, virtually no scattered light is observed. This is because any scattered light is absorbed by the dye in the bulk material prior to passing through the chip. However, we found that we could relate the intensity of the 532 nm light in the waveguide to the amount of autofluorescence generated by the dye. The waveguide attenuation can thus be determined by monitoring the decay in autofluorescence along the waveguide.

At 633 nm, we observe the expected linear relation between the optical power in the waveguide and distance, with the slope representing the propagation loss. However, at 532 nm we observe two attenuation regions. In Fig. 4B at 532 nm, we observe a period of high attenuation followed by a region of low attenuation. The first region represents the rate at which laser light is absorbed by the waveguide and as expected, the attenuation is high. However, the dye emits some of the absorbed energy as autofluorescence and a fraction of this light remains confined to the waveguide. Eventually the

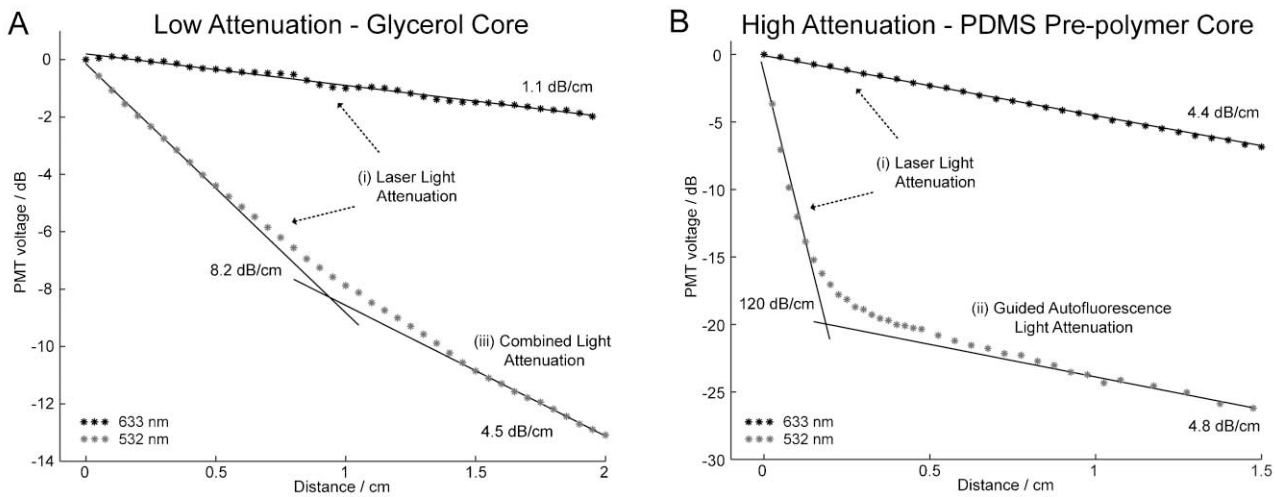

Fig. 4 Plot of the normalized intensity of light collected along the length of the waveguide. The propagation loss for dye-doped PDMS (1200 μg mL^{-1}) waveguides with (A) glycerol and (B) PDMS pre-polymer core materials are given after a diffusion time of 24 h. The losses at 633 nm remain low as compared to the attenuation at 532 nm and are constant over the test length. At 532 nm, the waveguide losses are significantly higher when the PDMS pre-polymer rather than glycerol is used as the core material. Three regions become apparent depending on the dominant source of light exiting the waveguide and this provides information on the spectral content of the waveguide (see text).

spectral content of the waveguide shifts from 532 nm to ~600 nm, the peak autofluorescence wavelength of the dye. This occurs at ~0.5 cm in Fig. 4B. At this point, the waveguide propagation loss closely matches the losses measured at 633 nm. We name these regions (i) laser light attenuation and (ii) guided autofluorescence light attenuation, respectively.

The propagation loss measurement of the lower attenuation waveguide (glycerol core) is provided in Fig. 4A. At 532 nm, the waveguide propagation loss does not level out to match the loss at 633 nm as it did in Fig. 4B. However, we believe that second linear fit is somewhere in the "knee" of the curve and that if our test waveguide was longer, we would eventually observe the losses to decrease to approximately 1.1 dB cm^{-1}. We term the region in the knee (iii) combined light attenuation since the spectral content in the waveguide is a combination of light at 532 nm and ~600 nm.

From Fig. 4B, we observe that a ~5 mm dye-doped waveguide filled with PDMS pre-polymer will provide similar performance to a commercial interference filter. A D590/55 m Chroma filter provides an attenuation of ~67 dB at 532 nm and ~80% light transmission at 590 nm whereas a ~5 mm dye-doped waveguide filled with pre-polymer (1200 μg mL^{-1}) provides an attenuation of 60 dB at 532 nm and ~60% light transmission at 633 nm. This is equivalent to Q-values of 4×10^6 and 6×10^5 for the dielectric filter and the waveguide filter, respectively. However, during operation, the small portion of the autofluorescence generated from the Sudan II dye that is confined within the detection waveguide is not efficiently removed by the integrated filter and becomes a source of background light at the photodetector. From Fig. 4B, we see that Sudan II autofluorescence limits the maximum performance of the waveguide filter to a Q-value of 1×10^2 or a difference in attenuation of 20 dB between the two curves.

3 Application: DNA fragment analysis

In order to demonstrate the effectiveness of the wavelength-selective waveguide, we compare the separation and detection of BKV PCR product using 4 different detection configurations (Fig. 5). The first two configurations use PDMS chips that have not been doped with the Sudan II dye to set a benchmark for comparison to the dye-doped chips. Configuration A (Fig. 5A) includes a clear, undoped PDMS chip with a commercial optical interference filter positioned in-line with the PMT. This configuration is identical to the waveguide system described in our previous work.[12] Configuration B (Fig. 5B) is identical to the benchmark except that the optical filter is removed from the system in order to quantify the noise-reduction provided by the commercial filter.

In configurations C and D, Sudan II dye-doped PDMS (1200 μg mL^{-1}) is used to replace the requirement for an external optical filter. In configuration C (Fig. 5C), the excitation fiber is inserted perpendicularly to the separation channel in a "buried optical fiber" configuration to prevent absorption of the excitation light before it can reach the sample. In this configuration, light leaves the excitation fiber and directly excites the sample without first passing through a waveguide. Sample fluorescence is then captured by the

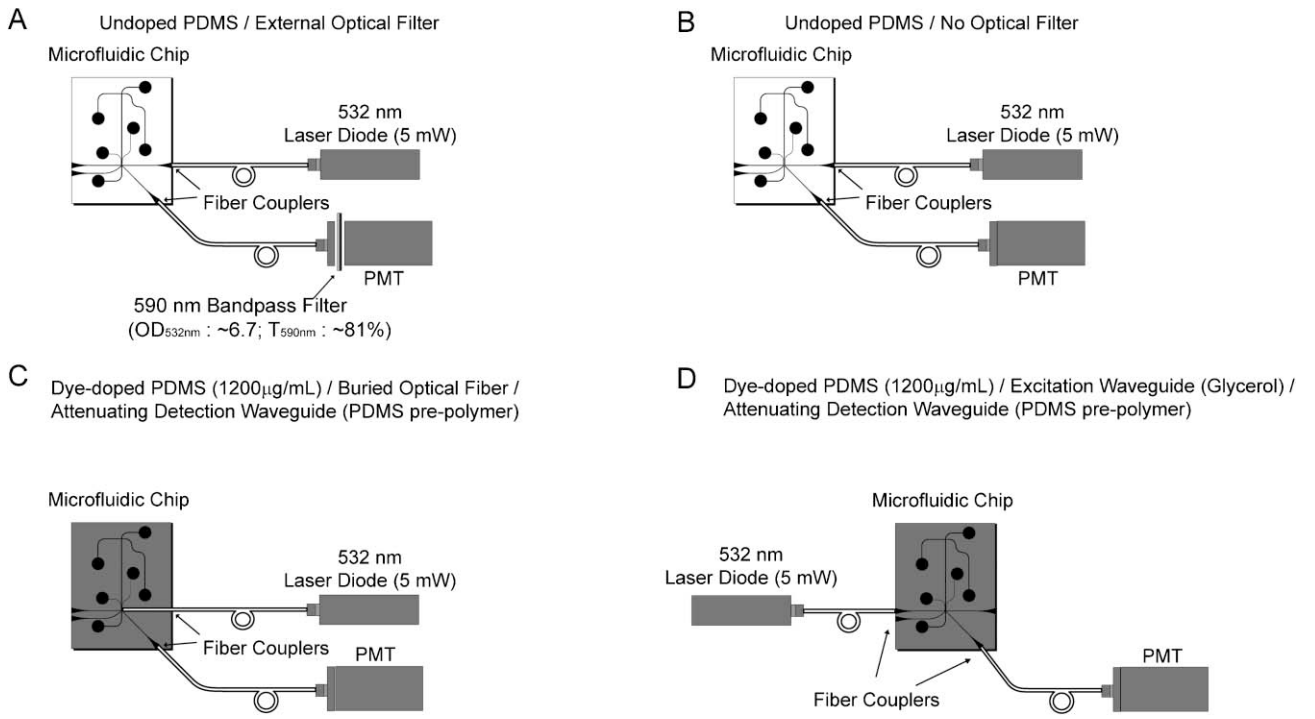

Fig. 5 Four optical detection scenarios are explored. (A) A colourless, undoped PDMS chip with a commercial external interference filter is used as a benchmark in this study. (B) The noise-reduction ability of the external filter is quantified by performing the same test as (A), but without the external filter. (C) By using a buried optical fiber for excitation, the optical filter properties of the attenuating waveguides are investigated without the influence of light absorption during the delivery of excitation light. (D) An all-waveguide solution. Low attenuation glycerol filled waveguides are used to deliver excitation light to the sample and detection is achieved using high attenuation PDMS pre-polymer attenuating waveguides.

detection waveguide and any collected excitation light is attenuated by the dye in the waveguide core. The buried optical fiber approach is not convenient since a fragile optical fiber must be fed into or encapsulated in the microfluidic chip. In configuration D (Fig. 5D), the excitation waveguide is filled with glycerol to reduce the diffusion of dye into the waveguide core (Fig. 1B). Since the waveguides used in the first three configurations are loaded using the same fluidic network, it is difficult to fill each waveguide with a separate material. In this configuration, the waveguides on the left side of the separation channel are loaded with glycerol and the waveguides on the right side with PDMS pre-polymer. Excitation light is delivered to the sample with a relatively small amount of attenuation since the glycerol reduces dye diffusion into the waveguide core and scatters less light than the PDMS pre-polymer. The sample fluorescence is collected by the opposing waveguide at an angle of 45° and any collected excitation light is absorbed by the attenuating waveguide.

The details on the microchip electrophoresis protocol can be found in our previous work.[12] In brief, new PDMS chips were conditioned with a solution of linear polyacrylamide (LPA—MW 600k–1000k) (Polysciences Inc., PA, USA) and Dynamic Coating (The Gel Co., CA, USA) prior to use for the first time to minimize surface effects. The absorptive polymer wall coating assists to suppress electroosmotic flow and the adsorption of analytes to the channel walls, both of which degrade the performance of the CE system. The PDMS chips were loaded with a sieving matrix (6% LPA), the sample well was loaded with 0.3 μL BKV PCR product and 2.7 μL 0.1 × TTE buffer (tris-taurine-ethylenediaminetetraacetic acid), while the remaining wells were loaded with 3 μL 1 × TTE buffer. The BKV PCR product is end-labelled with VIC dye (Applied Biosystems, CA, USA) and has a fluorescence emission peak at approximately 550 nm with a tail that extends into the red (~650 nm). Details of the BKV PCR product synthesis are described elsewhere.[17] DNA sample injection and separation was performed using a field of 158 V cm^{-1} for 100 s and 136 V cm^{-1} for 110 s, respectively. The injection time was reduced to 10 s for subsequent runs during the same experiment. The intersection between the waveguide and the microchannel is 11.5 mm from the injection point.

Except for configuration C, which uses a buried optical fiber for excitation, an excitation waveguide delivers light to the separation channel and the fluorescence is collected by a waveguide at an angle of 45° to the excitation waveguide (Fig. 5). The excitation and detection waveguides are each 5 mm in length. A 5 mW, 532 nm green laser diode (Holograms & Lasers Int., TX, USA) passes through an IR filter to remove any remaining 1064 nm light and is focused into the excitation optical fiber with 60% efficiency using a 10× microscope objective. Fluorescence is captured by the collection waveguide and is coupled into a second optical fiber that delivers light to a PMT (H5784-20, Hamamatsu, Japan). In configuration A (Fig. 5A), an in-line optical filter (D590/55 m, Chroma, VT, USA) is placed prior to the PMT. In all configurations, the PMT is sampled using an ADC at 48 kHz (NI USB-6008, National Instruments, TX, USA) and averaged in real-time to give an equivalent sample rate of 50 Hz.

The results from 3 chip runs using each of the outlined detection configurations is compiled in Table 2 and a comparison of typical DNA fragment separations is shown in Fig. 6. Configuration A (Fig. 5A) was our benchmark and this achieved the highest average SNR of 545. When the commercial external interference filter was removed, configuration B (Fig. 5B), we observed a factor of 60 reduction in the average SNR (SNR: 545 *vs.* 9) since a larger fraction of the excitation light reached the detector resulting in an increased signal baseline and detector shot noise.[12] The significance of the drop in SNR upon removal of the optical filter is observed by comparing the clear primer and product peaks of configuration A (Fig. 6A) with the barely discernable peaks of configuration B (Fig. 6B).

In configuration C (Fig. 5C), the undoped PDMS chip from configuration B is replaced with a dye-doped PDMS chip. A buried optical fiber approach is taken for excitation to prevent attenuation of the excitation light prior to sample excitation while detection is performed using an attenuating waveguide. An average SNR of 300 is observed with configuration C (without the use of an external optical filter), which is a 30-fold improvement over the similar configuration using the undoped PDMS (Fig. 5B) due to a large drop in the amount of excitation light reaching the detector and thus reduced shot noise. In configuration D (Fig. 5D), a low attenuation glycerol waveguide is used for excitation and a high attenuation waveguide PDMS pre-polymer waveguide is used for detection. Through this configuration, we gain an order of magnitude in terms of SNR as compared to configuration B (SNR: 138 *vs.* 9). In detection configurations without the use of an external optical filter, the improvement in SNR when using the dye-doped PDMS rather than undoped PDMS is clearly observed by comparing Fig. 6C, D to Fig. 6B. It is also observed that the addition of the Sudan II pigment into the

Table 2 Comparison of the SNR obtained from microchip CE runs using each waveguide LIF detection system. The noise and the baseline are calculated in the region immediately prior to the arrival of the product peak. The signal is an average of the background-corrected primer and product peak heights, where background-correcting involves subtracting the baseline from the measured peak height

		(A) Clear PDMS with external filter	(B) Clear PDMS without external filter	(C) Dye-doped PDMS without external filter[a]	(D) Dye-doped PDMS without external filter[b]
SNR: Signal-to-noise ratio	Run 1	521	12	338	127
	Run 2	508	6	339	88
	Run 3	607	10	231	198
	Average	**545**	9	**303**	**138**
	Std dev. (% of Avg)	**9.8%**	**29.7%**	**20.5%**	**40.6%**

[a] Excitation *via* buried optical fiber. [b] Glycerol excitation waveguide located on opposite side as detection waveguide.

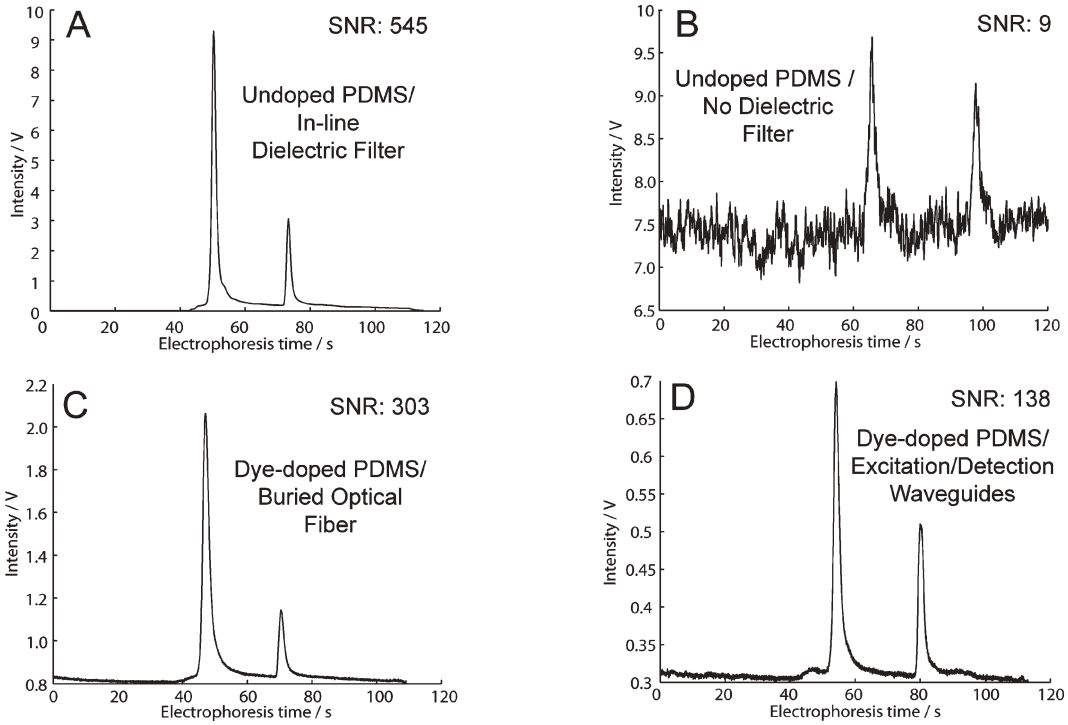

Fig. 6 The separation of the BK virus PCR product using each detection configuration. (A) Configuration A: The benchmark, undoped PDMS with an external optical filter, shows clear peaks with low noise. (B) Configuration B: The removal of the external optical filter results in a factor of 60 decrease in SNR and the peaks are difficult to detect. (C) Configuration C: When using dye-doped PDMS without an external optical filter, attenuating detection waveguides provide an optical filter effect providing a dramatic increase in SNR as compared to (B). (D) An all-waveguide approach within a dye-doped PDMS chip. Glycerol waveguides provide lower light attenuation at 532 nm during excitation and PDMS pre-polymer waveguide provide high attenuation at 532 nm during detection. The SNR is an order of magnitude larger than in (B). Since the glycerol excitation does exhibit non-negligible attenuation at 532 nm, the excitation power is lower than in configuration (C) resulting in a lower SNR.

PDMS microfluidic chip has no observable impact on other aspects of the separation, such as the peak resolution.

4 Conclusions

We have demonstrated that the incorporation of Sudan II dye into PDMS microfluidic chips can be used to create waveguides with built-in optical filters that are useful in removing excitation light while preserving the fluorescence signal during LIF. While a monolithic approach to sandwich a dye-doped chip between the source and detector would be a simple solution for a point-of-care diagnostic system, the optical density of the dye-doped PDMS may not be great enough to remove all of the excitation light prior to detection. Our new approach avoids this issue since the effective optical density of the attenuating waveguides can be increased by extending the length of the waveguide without a reduction in the amount of light captured by the waveguide. For a system that does not contain an external optical filter, we can improve the SNR by as much as 30 times using dye-doped PDMS. We have also shown that our wavelength-selective waveguide system provides results that are very comparable to our benchmark system, which relies on external optical filters. Thus a simplification in the detection system and a reduction in system cost can be achieved through the elimination of external optical interference filters and the use our novel dye-doped waveguide system.

There exist several usage options for the dye-doped waveguides. The waveguides could be filled immediately prior to use or they could be pre-filled. At high PDMS dye-loadings (1200 μg mL^{-1}) the waveguide displays high attenuation (118 dB cm^{-1}, 532 nm) after only 1 h when using a pre-polymer core, which is adequate for fluorescence sensing. This wait time could likely be further reduced while maintaining high sensitivity allowing the end-user to load the waveguides immediately prior to use. Loading the waveguides in advance, possibly during fabrication, would ensure the dye diffusion reaches steady-state prior to use. An alternative is to load the waveguide with liquid that contains the known steady-state dye concentration to suppress changes in dye concentration during operation.

While the dye-doped waveguides demonstrate similar attenuation to a commercial interference filter, autofluorescence of the dye currently limits the overall performance of the filter. The performance of the filter could be improved in future work by selecting a dye that generates less autofluorescence.

Acknowledgements

This work was supported in part by grants from the Natural Sciences and Engineering Research Council of Canada (NSERC), Canadian Institute for Photonic Innovations (CIPI), Alberta Ingenuity and the Informatics Circle of

Research Excellence (iCORE). We would like to thank Viet Hoang and Jana Lauzon for assistance with the PCR products, Alex Stickel and Dammika Manage for instrumentation and protocol support and the staff at the University of Alberta Nanofab for their valuable advice.

References

1 M. Dandin, P. Abshire and E. Smela, *Lab Chip*, 2007, **7**, 955–977.
2 M. A. Burns, B. N. Johnson, S. N. Brahmasandra, K. Handique, J. R. Webster, M. Krishnan, T. S. Sammarco, P. M. Man, D. Jones, D. Heldsinger, C. H. Mastrangelo and D. T. Burke, *Science*, 1998, **282**, 484–487.
3 J. R. Webster, M. A. Burns, D. T. Burke and C. H. Mastrangelo, *Anal. Chem.*, 2001, **73**, 1622–1626.
4 K. S. Shin, Y. H. Kim, J. A. Min, S. M. Kwak, S. K. Kim, E. G. Yang, J. H. Park, B. K. Ju, T. S. Kim and J. Y. Kang, *Anal. Chim. Acta*, 2006, **573**, 164–171.
5 Y. H. Kim, K. S. Shin, J. Y. Kang, E. G. Yang, K. K. Paek, D. S. Seo and B. K. Ju, *J. Microelectromech. Syst.*, 2006, **15**, 1152–1158.
6 V. Namasivayam, R. S. Lin, B. Johnson, S. Brahmasandra, Z. Razzacki, D. T. Burke and M. A. Burns, *J. Micromech. Microeng.*, 2004, **14**, 81–90.
7 K. S. Shin, Y. H. Kim, K. K. Paek, J. H. Park, E. G. Yang, T. S. Kim, J. Y. Kang and B. K. Ju, *IEEE Electron Device Lett.*, 2006, **27**, 746–748.
8 K. S. Shin, S. W. Lee, K. C. Han, S. K. Kim, E. K. Yang, J. H. Park, B. K. Ju, J. Y. Kang and T. S. Kim, *Biosens. Bioelectron.*, 2007, **22**, 2261–2267.
9 O. Hofmann, X. H. Wang, A. Cornwell, S. Beecher, A. Raja, D. D. C. Bradley, A. J. deMello and J. C. deMello, *Lab Chip*, 2006, **6**, 981–987.
10 M. L. Chabinyc, D. T. Chiu, J. C. McDonald, A. D. Stroock, J. F. Christian, A. M. Karger and G. M. Whitesides, *Anal. Chem.*, 2001, **73**, 4491–4498.
11 J. A. Chediak, Z. S. Luo, J. G. Seo, N. Cheung, L. P. Lee and T. D. Sands, *Sens. Actuators, A*, 2004, **111**, 1–7.
12 C. L. Bliss, J. N. McMullin and C. J. Backhouse, *Lab Chip*, 2007, **7**, 1280–1287.
13 D. B. Wolfe, D. V. Vezenov, B. T. Mayers, G. M. Whitesides, R. S. Conroy and M. G. Prentiss, *Appl. Phys. Lett.*, 2005, **87**, 181105.
14 D. Yin, D. W. Deamer, H. Schmidt, J. P. Barber and A. R. Hawkins, *Appl. Phys. Lett.*, 2004, **85**, 3477–3479.
15 K. S. Lee, H. L. T. Lee and R. J. Ram, *Lab Chip*, 2007, **7**, 1539–1545.
16 E. Hecht, *Optics*, Addison Wesley, San Francisco, CA, USA, 4th edn, 2001.
17 G. V. Kaigala, R. J. Huskins, J. Preiksaitis, X. L. Pang, L. M. Pilarski and C. J. Backhouse, *Electrophoresis*, 2006, **27**, 3753–3763.